Automatic Layout Optimization of an EMC filter

Thomas DE OLIVEIRA, Jean-Luc SCHANEN, Jean-Michel GUICHON, Laurent GERBAUD
G2ELab (UMR 5269 INPG-UJF-CNRS), Bat Ense3, B.P.46
38402 St Martin d'Hères CEDEX France

Abstract- The transfer function of an EMC (Electro-Magnetic Compatibility) filter is strongly disturbed in high frequency due to stray electromagnetic phenomena. On the one hand the imperfections of the components but also all magnetic couplings on the other hand. Although these effects seem to be negative, it is possible to reduce the impacts of these imperfections on the filter response, and even to use them in order to improve its behavior. A proper arrangement of components and a clever layout of tracks are required. Nevertheless, the complexity of the problem makes unthinkable a manual construction. Therefore, this paper discusses the implementation of an automatic routing algorithm based on the PEEC method (Partial Equivalent Element Circuit), in order to consider the electro-magnetic aspect in the layout definition.

I. INTRODUCTION

The general trend in power electronics is to develop always more compact systems, especially for embedded applications. When looking on a power converter, the EMC filter represents 30% of the volume: there is thus a strong need to focus on this part. Furthermore, with the integration and increased compactness, the distances between the components are so small that stray electromagnetic interactions become no more negligible. Therefore, the filter behaviour can be dramatically depreciated, since uncontrolled stray interactions impact on the transfer function. Some authors have already experienced and reported these phenomena in the literature [1], and even proposed some guidelines for component placement and the associated layout [2-3]. This work proposes some models to better analyse these stray interactions, using a rooting method, based on PEEC representation. Currently, the existing routing algorithms are limited, either to find the layout of tracks so as to minimize their length (*geometric criterion only*), either to design the tracks in order to avoid areas of strong magnetic field, and thus to limit the magnetic couplings between components and tracks [4]. The main advantage of the process presented in this paper, is that it allows using the phenomena usually neglected or restricted. They are so many magnetic elements to consider, that a manual construction is unthinkable. The realization of an automatic routing algorithm is so required. It must be able to consider the electro-magnetic aspects during the routing research. To do so, it will be built on the PEEC bases [5-6], which allows accounting for the imperfections of components, as well as stray magnetic couplings. To be noticed that in this paper, *the electro-static coupling phenomena will not be considered*

Section II will briefly introduce the filter used for application. The component models using PEEC representation will be detailed in section III and validated in section IV. The algorithm for the automatic layout generation, based on a variation of Lee & Dijkstra algorithms [7-9], will be used in section V.

II. STUDIED FILTER

In order to limit the complexity of the system, we focused our works on a low-pass filter. This does not modify the generality of the method. The filter topology is similar to that of a conventional differential mode filter (*Figure 1*); the only difference is the common ground of input/output ports. This is for simplicity reasons, since the transfer function using a network analyzer will automatically ground the input and the output, except if an insulation method (balloon) is used.

The capacity of each ''Cx'' plastic capacitor is 680nF. Their identifications have been realized with an impedance meter device (*HP 4194*), by averaging the measurements of a sample of 10 identical capacitors.

The average capacity calculated was 640,717nF, with an average ESL (*Equivalent Series Inductor*) 9,4nH, and an average ESR (*Equivalent Series Resistor*) 21,6mΩ. The filter inductor has been built on a magnetic iron powder core (*μr≈60*), and the inductance is about 15µH by coil. Both windings are wound on a single magnetic core. The two wirings of the Differential Mode inductor have been identified separately, accounting for internal resonance (up to roughly 10MHz) by adding stray winding capacitance. After identification, an equivalent circuit of the filter has been obtained, accounting for all stray elements of the filter components (Fig.1.).
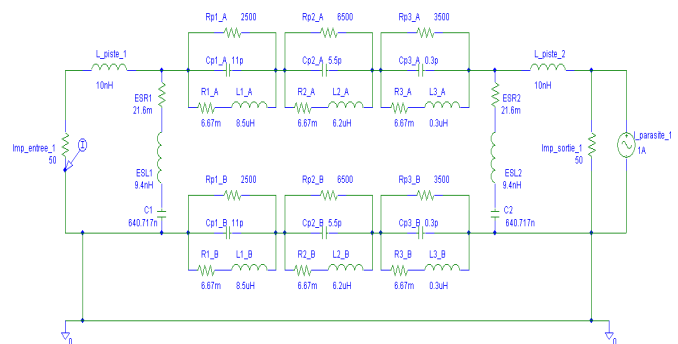

Figure 1. Equivalent circuit of the low-pass filter

III. COMPONENTS MODELING

The aim of this section is to provide a modeling method, able to account for magnetic couplings of the components with the rest of the circuit (tracks, other components, …). For this purpose, PEEC method will be used [10-13].

A. Advantage of the PEEC method

The PEEC method is an integral method which allows treating complex geometries, by meshing the conductors only, and not the air around [5 - 6]. The quick computation times allows optimization [10]. Usually, this method is used to model only tracks or cables. Regarding our system, we have to model discrete components too, to take into account all stray magnetic couplings. Obviously, some simplifications are required for each model, because it is impossible to build exactly the internal geometries of components.

B. Capacitor PEEC modeling

The internal structure of plastic capacitors is represented in Fig.2. It is composed of a metallized wounded film. The edges of this film are also metallized, composing the capacitor access to all electrodes. The internal geometry of a ''Cx'' capacitor is so complicated, that it is impossible to model it exactly. We choose therefore to define a simplified model, using a kind of "homogenization method", by replacing the thousands of conductive/insulation layers by only few ones, and using an equivalent resistivity. This is basically the same idea as the Dowell approximation [11].

So, we have established our first model on this base, limiting only the number of equivalent electrodes to 5 (Fig. 3). This is just a compromise between an easy and correct modeling, and an acceptable simulation time. The external dimensions remain of course similar compared with those of the real component.

Three parameters are available to tune the model: the equivalent resistivity of the electrodes ρ, their equivalent thickness "t" and the spacing "k" defining the overlap between the two groups of electrodes. The equivalent series inductance ESL has been chosen to check the result of the tuning of the model, since it is representative of the magnetic behavior of the component. It will also be shown that this model is good to account for magnetic couplings as well.

Figure 4.a shows the variations of ESL according to the electrodes resistivity and their thickness. Figure 4.b illustrates the variations of ESL as a function of the distance ''k''.

The set of parameters allowing the best fit to the averaged identified ESL of the real component is defined by:

$$\rho = 7,3.10^{-5} \ \Omega.m$$
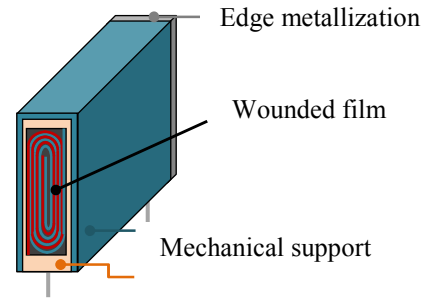
$$k = 8,125 \ mm$$

$$t = 0,85 \ mm$$

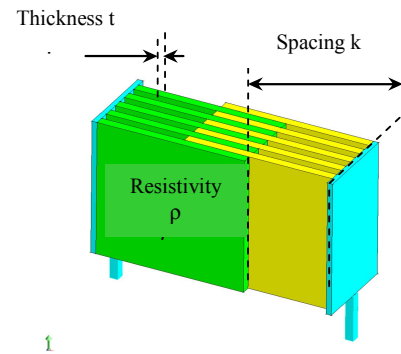Figure 2. Internal structure of a real ''Cx'' capacitor

Figure 3. First model of a ''Cx'' capacitor
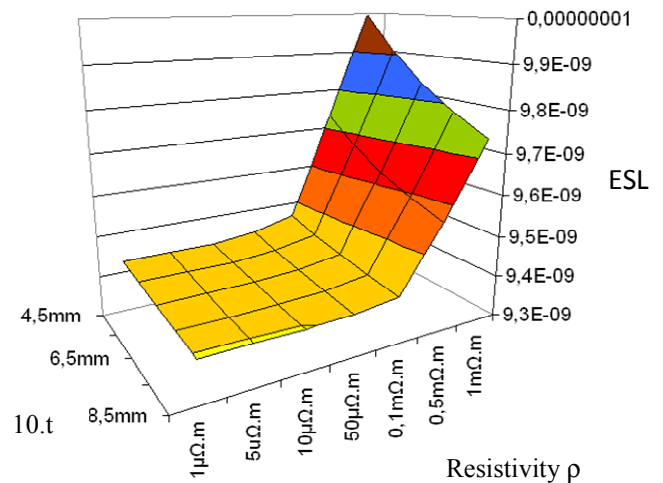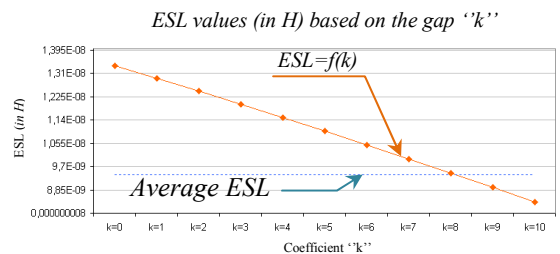

Figure 4.a. ESL[H]=f(t, ρ)

Figure 4.b. ESL=f(k)

In order to validate the model on the magnetic coupling aspect, we used a two parallel capacitors system. The two components are associated as illustrated in Fig.5. The distance between the two components is variable in order to increase or not the coupling between them. Six positions are thus possible for the mobile capacitor. To emphasize the validity of our model, we considered the position for which the coupling between components is the strongest, and so when the two capacitors are the closest.

To account for the track impedance, we modeled them, using PEEC, but without accounting for the coupling between the capacitors and them. The calculated total inductance was 15,8nH. It results from the combination of the two ESL and the tracks impedance. A complete PEEC simulation has then been carried out, using the PEEC capacitor models and the tracks representation. The equivalent inductance of the paralleled association has now been changed to 12.6nH, what was also obtained in experiment. The 3.2nH difference is therefore linked to the stray magnetic couplings between components themselves, and between components and tracks. Figure 6 presents the behavior of the complete simulation, in comparison with the experimental results: the physic of the component is well represented.

The previous validation shows clearly that PEEC modeling is a good way to account for the magnetic behavior of the capacitor. However, the model built remains too heavy regarding simulation time, if we want to use it in an optimization process. So we have built a second model, based on the same principle. The internal geometry of a capacitor is thus assimilated to a single electrode, directly connected with both metallizations (Fig. 7.). A gap ''k'' between one side of the electrode and one metallization is still configurable, and it is one of the fitting parameter. The second one remains the resistivity of the electrode ''ρ''.

The identified model fitting best the ESL value of the actual component, is defined by:

$$\rho = 1{,}25.10^{-4} \ \Omega.m \qquad\qquad k = 4{,}5 \ mm$$

Table 1 summarizes the characteristics of every modeling, compared with those of the ''Cx'' real capacitor.

Table 1: Summary of models characteristics

	ρ (Ω.m)	k (mm)	e (mm)	ESR (mΩ)	ESL (nH)
Real capacitor				21,6	9,4
First modeling	$7{,}3.10^{-5}$	8,125	0,85	21,576	9,399
Simplified modeling	$1{,}25.10^{-4}$	4,5		20,9	9,37

The same validation procedure has been carried out for this simplified model. The total inductance of the paralleled association has been evaluated at 13nH instead of 12,6nH. The results of the complete model using the simplified representation are shown on Fig. 8. Therefore, it can be shown that lightened models are also correct.
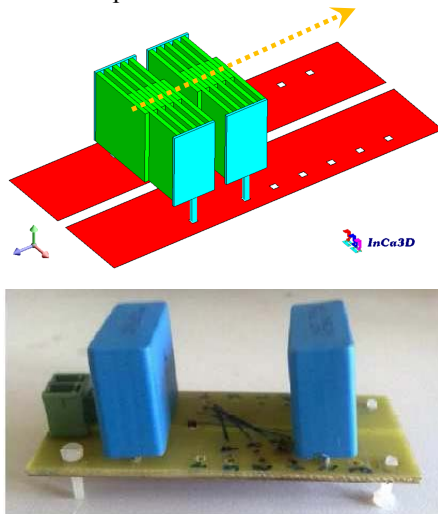

Figure 5. Validation of the capacitor model using two paralleled capacitors
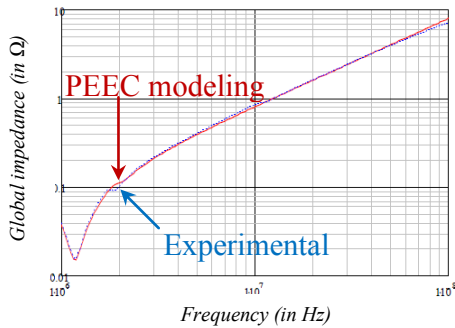
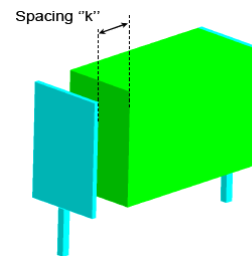Figure 6. Experimental impedance measurement (blue), and with the PEEC modeling (red)

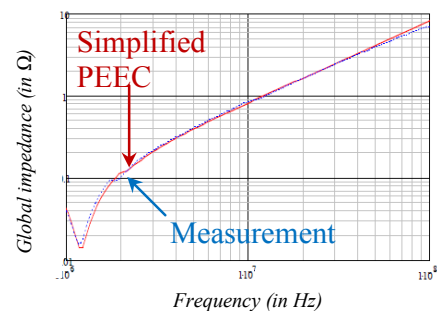

Figure 7. ''Cx'' capacitor simplified model

Figure 8. Experimental impedance measurement (blue), and with the PEEC modeling (red)

C. Inductor PEEC model

Accounting for an inhomogeneous medium in the PEEC environment is currently difficult and would result in huge problems. Therefore, the magnetic material has not been taken into account. Fortunately, the limited influence of magnetic materials on stray magnetic fields has already been shown in previous studies [4, 12]. It is thus possible to neglect the magnetic core in the modeling. Obviously, the inductance will have to be modified since the magnetizing part is not taken into account, but all leakage effects, including the magnetic coupling, will be considered, and this is the main goal of the study.

For validation purpose, we investigated the magnetic coupling between the inductor itself and a receiving loop located in the vicinity. Several materials have been used for the core, in order to analyze the impact on the magnetic coupling. One for which its permeability is equal to zero (*plastic, μ=μo*), and the original one (*iron powder, μr≈60*).

The mutual coupling measurement has been measured as follows: the two coils connected in series, are powered by a current source with a variable frequency. For each frequency, the induced voltage at the terminals of the receiving loop is measured. Therefore, the coupling ''$M_{L\text{-}ReceivingCoil}(f)$'' can be deduced. The experiment is presented on Fig.9-a, and the results displayed in 9.b, for the particular case where the test loop is just under the inductor (Fig.10). Some differences appear in high frequency due to electrostatic phenomena between coils themselves, and between the coils and the magnetic core.
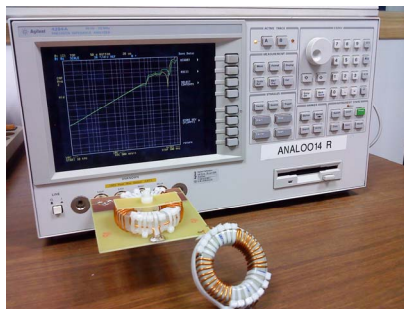

Figure 9.a. Experimental setup to measure the magnetic coupling with a receiving loop located below the inductor
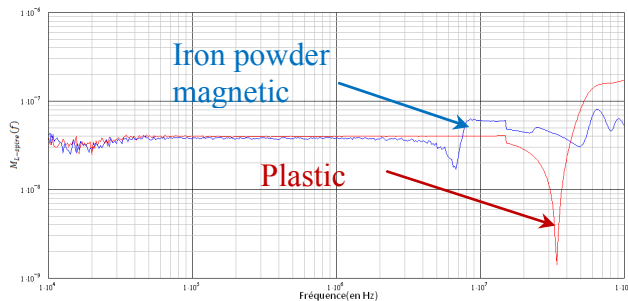

Figure 9.b. Measures of coupling with a receiving loop located below the inductor (results)
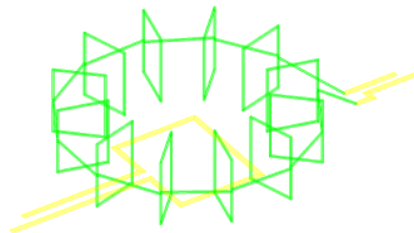

Figure 10. Modeling of the inductor without accounting for the magnetic material. Note the receiving loop below. Note also the particular way of winding chosen for realization, in order to simplify the modeling.

From experimental results at low frequencies (*below 5MHz*), where the magnetic behavior is dominant, it is clear that the mutual coefficient are identical. Therefore, a PEEC modeling neglecting the magnetic core can be used to represent the coupling [4, 12].

However, even if the results of this model are very good, the complexity of the PEEC model is very high, and this will not allow any optimization. Therefore, a simplified representation has been proposed. It uses a simple loop, corresponding to the current displacement turn after turn (Fig.11). This model is very simple, with a reasonable accuracy, as illustrated in Table 2.

To validate this simple representation, we measured the magnetic coupling between the inductor and the test loop. We achieved the same operation with our PEEC modeling. Table 2 summarizes de results at a 10 kHz frequency (when the impact of the magnetic material is negligible) regarding magnetic leakages.

Table 2: Summary of models characteristics

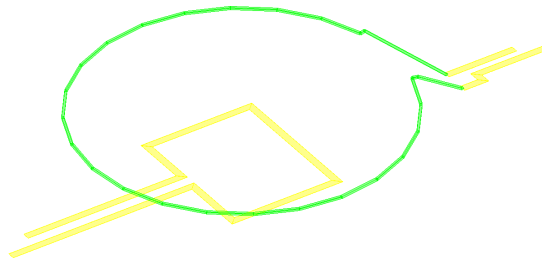|	Iron powder torus	Plastic one	PEEC modeling
Experimental measurements	10,8 nH	10,9 nH	
Complete PEEC modeling			9,8 nH
Simplified PEEC modeling			9,9 nH

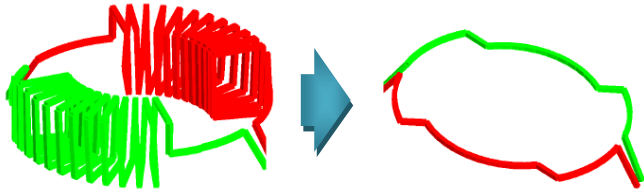Figure 11. Simplified PEEC model of an inductor

Figure 12. Simplified filter inductor model

Applying this method to the DM filter inductor leads to the result of Fig.12, which is far simpler than the complete one. It will be usable in an optimization process, in combination with the simplified model of the capacitors and the PEEC models of the tracks. This will be detailed in the next section.

IV. PEEC MODELS VALIDATIONS

In order to validate the previous PEEC models in a complex environment, including several components and all tracks (also represented with a PEEC model), we built three different topologies for our previous low-pass filter (Fig. 13). The magnetic couplings between components are more or less favored by topology. We then measured the transfer function (*Rohde-Schwarz ZVRE*) for every filter, to compare them one by one with the equivalent PEEC filter model, complete PEEC model and simplified model (Fig. 14).
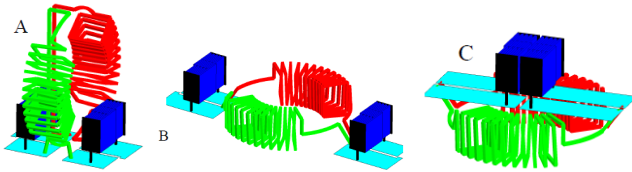

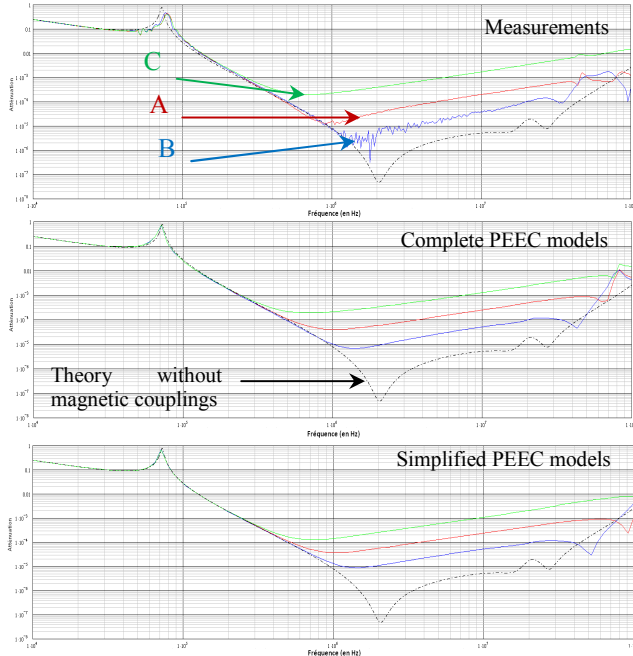Figure 13: Different topologies of our low-pass filter

Figure 14: Transfer function for each topology of low-pass filter built

It can therefore be noticed that the behavior of both full and simplified PEEC model remain relatively close to the responses of real filters until roughly 20 MHz. Beyond this frequency, electrostatic phenomena -not taken into account in the PEEC environment- alter the physical behavior of filters.

V. AUTOMATIC ROUTING ALGORITHM

Once the PEEC models have been validated, it is possible to use them in an optimization process. The chosen algorithm relies on the same bases than the existing ones [7-9]. The path between two points is defined by a weight, either governed by the geometry, either by another parameter. Regarding the convergence rapidity, this algorithm does not search the best path but one of the best. This procedure is taken from the Astar (*A**) algorithm (*a variant of the Dijkstra algorithm [8]*), and it limits the number of possible solutions analyzed.

Usually, the graph theory applied to the rooting strategy is governed by geometrical criteria. Here it is necessary to introduce the electromagnetic behavior. However, the problem is that this behavior can only be known once the layout has been completely defined, and not during the optimization process. All the weights can thus be defined if the global electromagnetic radiation is known, included tracks. In other words, the tracks are necessary to set the weights required to find them. It is therefore an endless problem since the layout must be known to set the weights.

The first algorithm that we have built uses a random parameter, which allows testing several different possible solutions, and keeping only the best found. An evolution of this random process has then be written so that to lead and to speed up the research of an optimized solution. This second process is based on genetic algorithms. The principle is to test a first family of mother solutions randomly generated, to keep only the ''N'' best ones. ''X'' girl solutions have then been created with those best solutions, by modifying only one point of a track (*point randomly chosen*) for every ''N'' mother solutions. Henceforth, that new family is analyzed in order to keep the ''N'' new best solutions, which become the new mother ones. And the process keeps on in this way to converge towards an acceptable solution.

We applied these two algorithms to the example of the low pass filter, for the two components locations "A" and "B" of Fig.13. The components are disposed at fixed coordinates, and the rooting algorithm will search the best track layout to reach a given objective. A simple objective function was chosen: achieving the lowest gain at a given frequency. This frequency has been fixed at 10MHz, in the frequency range where no stray resonance appears. Obviously, more complex objective functions could have been checked, by increasing the number of tested frequencies for instance, but for demonstration purpose, this first step has been considered sufficient.

Figure 15 presents the initial geometry for case "A", and Fig.16 shows one of the optimized results.
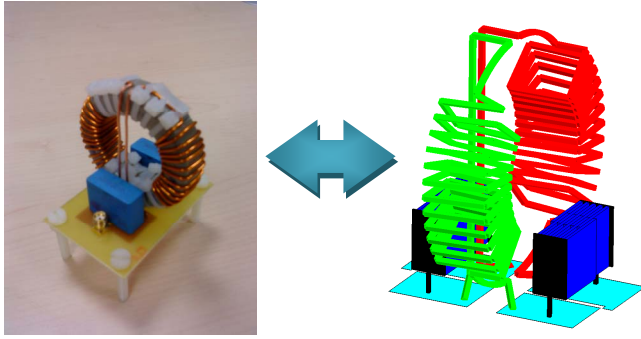
Figure 15. Low-pass filter with the component location of case "A" and non optimized tracks
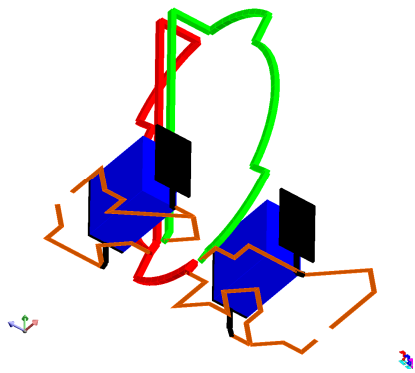

Figure 16. Low-pass filter with the component location of case "A" and optimized tracks

Figure 17 summarizes the transfer functions of the initial filter (Fig.15) and the optimized filter. The pure random algorithm result is compared with the genetic one.

We also added a further simplification for the inductor representation: instead of an equivalent circular loop for the inductor, we replaced it by an equivalent polygon, which is far simpler to be modeled by PEEC method. The accuracy is still fair, with a large reduction in computation time.

The numerical results (used as objective function) have also been summarized in table 3.

Table 3: Summary of the attenuations at 10MHz for every optimized solution

	Attenuation at 10MHz
Standard routing (*larges tracks*)	-74 dB
Solution got with the 1st algorithm(entirely random)	-97 dB
Solution got with the 2nd algorithm (*genetic*)	-112,4 dB
Solution got with the 2nd algorithm, and with a simplified inductor definition (*equivalent loop not circular but polygonal*)	-112,6 dB

— · — · — Theory without magnetic couplings

———— Measurement

———— Complete PEEC models

———— Simplified PEEC models

— — — Optimized routing by the 1 first algorithm (*entirely random*), and got after 16 hours and 300 attempts (*with a standard computer CPU 2GHz and 3GB of RAM*)

— — — Optimized routing by the 2nd algorithm (*genetic*), and got after 18 hours

— — — Optimized routing by the 2nd algorithm and with a simplified inductor definition (*equivalent loop not circular but polygonal*). Routing got after only 5 hours instead of 18 hours.
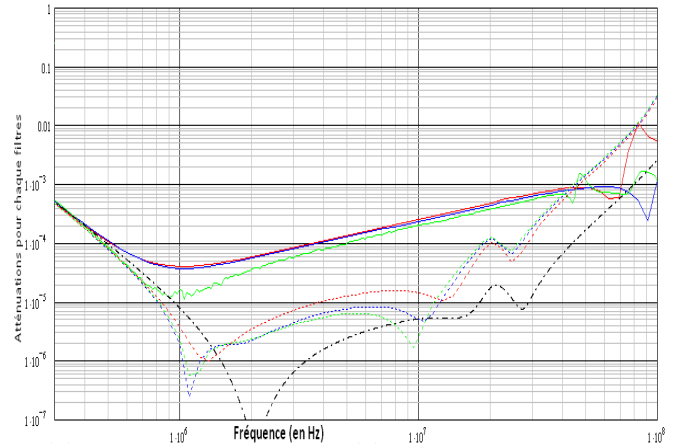

Figure 17. Transfer functions for a low-pass filter with the component location of case "A"

As we can notice, the transfer functions of the optimized solutions are better compared with the initial filter response. Moreover, it can be outlined that at some MHz, the optimized solutions behaviors are still better than the theory without any magnetic coupling. The possibility to use those electro-magnetic phenomena properly is thus clearly illustrated.

Figure 18 illustrates how the two algorithms converge to the final solution. It is obvious that the pure random algorithm is not as efficient as the genetic one.
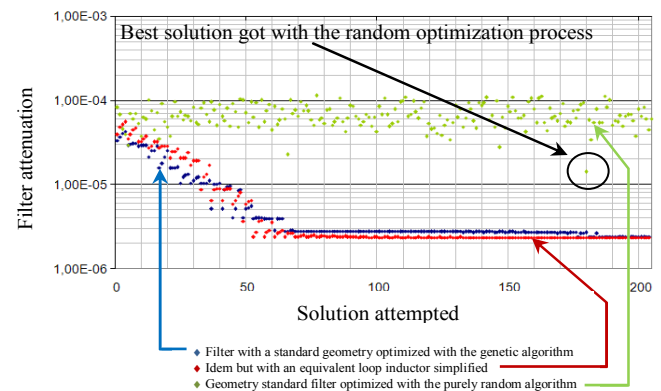

Figure 18. Evolution of the routing solutions attempted

Nevertheless, it is necessary to have sufficient magnetic coupling in order to be able to optimize the filter with the layout of the tracks. In order to illustrate this remark, the case of the component location "B" has been considered. In this case, the components are so far away, and the coupling between them is so small, that the optimization procedure could not improve the layout further. Indeed, the optimized solutions (Fig.19) have almost the same behavior than the original filter (Fig.20).
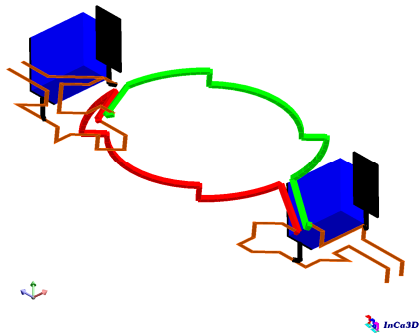

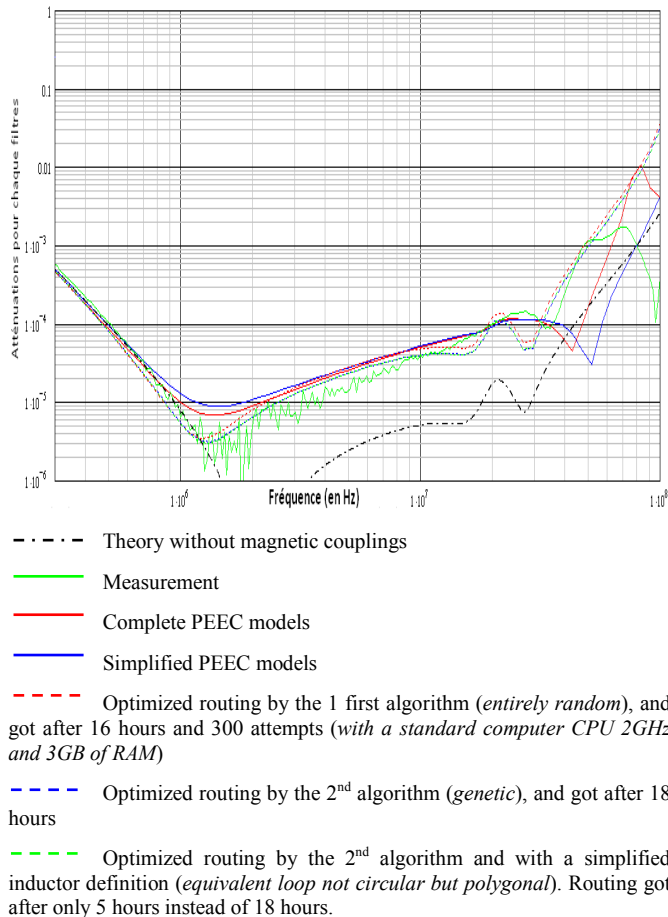Figure 19. Low pass filter minimizing the magnetic couplings between components

– · – · – Theory without magnetic couplings

――――― Measurement

――――― Complete PEEC models

――――― Simplified PEEC models

– – – – Optimized routing by the 1 first algorithm (*entirely random*), and got after 16 hours and 300 attempts (*with a standard computer CPU 2GHz and 3GB of RAM*)

– – – – Optimized routing by the 2nd algorithm (*genetic*), and got after 18 hours

– – – – Optimized routing by the 2nd algorithm and with a simplified inductor definition (*equivalent loop not circular but polygonal*). Routing got after only 5 hours instead of 18 hours.

Figure 20. Transfer functions for a low-pass filter minimizing some couplings

VI. CONCLUSION

The originality of our study is to present the possibility to use the stray magnetic couplings to optimize the system. To do so, we propose through that paper, a PEEC method which allows a behavior improvement based on a smart layout of the tracks. This method requires some PEEC models of discrete components, whose impedance well as electro-magnetic radiation remain similar with the physic of the real component.

VII. REFERENCES

[1] Eckart Hoene, "EMC in Power Electronics", CIPS 2008, Nurenberg, Germany

[2] Shuo Wang; Lee, F.C.; van Wyk, J.D., "A Study of Integration of Parasitic Cancellation, Techniques for EMI Filter Design With Discrete Components", Power Electronics, IEEE, Transactions on, Volume 23, Issue 6, 2008

[3] Timothy C. Neugebauer, Joshua W. Phinney, David J. Perreault, "Filters and Components with Inductance Cancellation", IEEE 2002, MIT, Cambridge USA

[4] Hoene, E.; Lissner, A.; Guttowski, S. "Prediction of EMI behaviour in terms of passive component placement", EMC Zurich 2007. 24-28 Sept. 2007

[5] Ruehli, A.E.; Antonini, G., "On modeling accuracy of EMI problems using PEEC", Electromagnetic Compatibility, 2003 IEEE International Symposium on, Volume 1, Issue , 18-22 Aug. 2003

[6] Vincent Ardon, Jérémie Aimé, Olivier Chadebec, Edith Clavel, Enrico Vialardi, "MoM and PEEC Method to Reach a Complete Equivalent Circuit of a Static Converter", EMC Zurich 2009, Switzerland, jan 2009

[7] C. Y. Lee, "4n Algorithm for Path Connections and Its Applications", IRE Trans. on Electric Computers, 1961

[8] E. W. Dijkstra, "A note on two problems in connexion with graphs, "Numer. Math., vol. 1, pp. 269-271, 1959

[9] F.Rubin, "The Lee path connection algorithm", IEEE Trans. On Computers, VOL. c-23, No. 9, 1974

[10] C.Martin, JL.Schanen, JM.Guichon, R.Pasterczyk, "Analysis of Electromagnetic Coupling and Current Distribution inside a Power Module ", IEEE trans on IAS – July/August 2007, vol. 43, no. 4

[11] DowellP.L., "Effect of eddy currents in transformer windings",Proceedings IEE, Vol.133, n°8, 1966.

[12] T.DeOliveira, JM.Guichon, JL.Schanen, L.Gerbaud, "PEEC-Models for EMC filter layout optimization", CIPS 2010, Nuerenberg, Germany

[13] InCa software – http://www.cedrat.com/en/software-solutions/inca3d.html